REFERENCES

[1] I. Nishi, K. Yanagisawa, and T. Toshima, "Spiral resonator for PCM-400 M system," *Rev. Elect. Comm. Lab.*, vol. 24, nos. 9–10, pp. 776–786, 1976.

[2] A. Olivei, "Optimized miniature thin-film planar inductors compatible with integrated circuits," *IEEE Trans. Parts, Hybrids, Packag.*, vol. PHP-5, pp. 71–88, June 1969.

[3] Y. Midorikawa, I. Marinova, S. Hayano, and N. Yaito, "Electromagnetic field analysis of film transformer," *IEEE Trans. Magn.*, vol. 31, pp. 1456–1459, May 1995.

[4] M. Caulton, S. P. Knight, and D. A. Daly, "Hybrid integrated lumped-element microwave amplifiers," *IEEE Trans. Electron Devices*, vol. ED-15, pp. 459–466, July 1968.

[5] R. S. Pengelly and D. C. Richard, "Design, measurement and application of lumped elements up to J-band," in *Proc. 7th Europ. Microwave Conf.*, Copenhagen, Denmark, 1977, pp. 460–464.

[6] K. C. Gupta, R. Garg, and R. Chadha, *Computer-Aided Design of Microwave Circuits*. Norwood, MA: Artech House, 1981, pp. 211–212.

[7] R. Chadha and K. C. Gupta, "Green's functions for circular sectors, annular rings and annular sectors in planar microwave circuits," *IEEE Trans. Microwave Theory Tech.*, vol. 29, pp. 68–71, Jan. 1981.

[8] A. J. Palermo, "Distributed capacity of single layer coils," *Proc. IRE*, vol. 22, pp. 897–909, 1934.

[9] R. E. Harrington, *Field Computation by Moment Methods*. Malabar, FL: Krieger, 1985, p. 27.

[10] J. M. Schallenberg, "CAD models for suspended and inverted microstrip," *IEEE Trans. Microwave Theory Tech.*, vol. 43, pp. 1247–1254, June 1995.

Design of Modified Phase Reversal Electrode in Broad-Band Electrooptic Modulators at 100 GHz

Kwok-Wah Hui, B. Y. Wu, Y. M. Choi, J. H. Peng, and K. S. Chiang

***Abstract*—An analysis is given on the modified phase reversal structure of electro-optic modulators. It is shown that the bandwidth to half-wave voltage ratio (BVR) increases with the number of phase reversal sections. Under the assumption that the number of electrode sections is M, a set of M-elements second-order nonlinear equations has been derived and solved by Newton's iteration method. The calculated results provide the optimum overlap integral for each section of a phase reversal modulator in order to "flatten" the frequency response of the device.**

***Index Terms*—Integrated optics, optical modulators, optimization.**

I. INTRODUCTION

The bandwidth of integrated electrooptic modulators is limited mainly by the transmission attenuation and the mismatch between the optical and microwave velocities [1]–[3]. To increase the bandwidth, the length of the electrode needs to be reduced. This will, however, in turn increase the half-wave voltage, V_π [4]. In the past few years, a number of modulators have been built using techniques such as "thick electrode" and "ridge structure" to eliminate the velocity mismatch between optical and microwave signals [5], [6]. Although in these modulators the length of the electrode can be increased to maximize the response of the device, their electrode structures are rather complicated and would be more difficult to fabricate. An alternative to increase the BVR is the use of the phase reversal electrodes [7]. There are different types of phase reversal electrodes [8], [9]. These include the periodic and nonperiodic types, the continuous function, and the simple step function electrodes. Each of them provides a certain degree of improvement on the flatness of the frequency response with significant increase in bandwidth to half-wave voltage ratio (BVR) [10]. This paper will concentrate on the nonperiodic step function electrode because it has a flat frequency response and is easier to fabricate when compared with the continuous function electrode, thick electrode, and ridge structure. The electrode is divided into M sections of equal length. Mathematical analysis yields a set of M-elements second-order nonlinear equations that is then solved by Newton's iteration method. The figure of merit, Q, can then be computed. Here, Q is defined as the ratio of the BVR for an electro-optic modulator with M sections of electrodes to that of a conventional electro-optic modulator (with only one section of electrode).

Manuscript received December 4, 1995; revised September 23, 1996.

K.-W. Hui and K. S. Chiang are with the Department of Electronic Engineering, City University of Hong Kong, Hong Kong.

B. Y. Wu and J. H. Peng are with the Department of Electronic Engineering, Tsinghua University, Beijing, China.

Y. M. Choi is with the ISO-Ing Centre, Hong Kong.

Publisher Item Identifier S 0018-9480(97)00279-2.

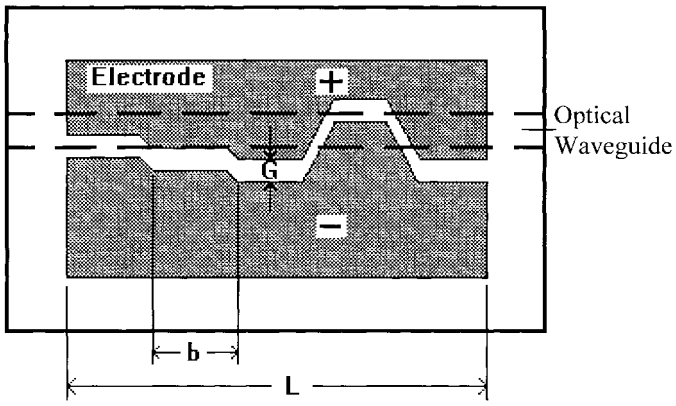

Fig. 1. Schematic diagram of phase modulator with five sections of phase reversal electrode.

II. ELECTRODE STRUCTURE

Fig. 1 shows the schematic diagram of a five-section phase modulator. An electrode of length L is divided into M sections of equal length. The length of each section, b, is, therefore, equal to L/M. This structure employs a simple step function and provides a flat frequency response. The electro-optic overlap integral at the ith section is Γ_i where $i = 1, 2, \cdots, M$. In general, different sections of i have different Γ_i since the relative position between the central line of the electrode gap, G, and that of the optical waveguide varies in different sections. The relative position between the central lines in each section, however, is constant. This type of electrode pattern is called the step electrode structure.

III. MATHEMATICAL ANALYSIS

For a phase reversal structure in which the microwave phase is reversed at the end of each section, the total induced optical phase shift ϕ is given by [8]

$$\frac{\phi(f)}{FL} = \frac{1}{\gamma L}\sum_{i=1}^{M}\Gamma_i\left[e^{-\gamma(i-1)b} - e^{-\gamma ib}\right] \tag{1}$$

where

$\phi(f)$ function of the modulating frequency, f_m;
F $= (-n_o^3 r E_m \pi/\lambda)\exp(j\omega t_0)$;
n_o effective refractive index for the optical wave;

r	electro-optical coefficient of the crystal;
E_m	amplitude of the microwave modulating electric field;
λ	optical wavelength;
L	electrode length;
γ	$= \alpha + j\beta'$ propagation constant;
α	attenuation coefficient;
β'	$= 2\pi f(n_m - n_o)/c$ phase constant;
n_m	effective refractive index for the modulating microwave;
c	velocity of light in free space.

Assuming that $\alpha = 0$, the overlap integral Γ_i is given by

$$\Gamma_i = \frac{G}{V}\frac{\int_{-\infty}^{+\infty}\int_{-\infty}^{+\infty} E_{\mathrm{mi}}(x,y)[\varepsilon(x,y)]^2 dxdy}{\int_{-\infty}^{+\infty}\int_{-\infty}^{+\infty}[\varepsilon(x,y)]^2 dxdy}$$

where

G	distance between the electrodes;
V	voltage between the electrodes;
$E_{\mathrm{mi}}(x,y)$	transverse electric field distribution of the microwave at the ith section;
$\varepsilon(x,y)$	transverse electric field distribution of the optical wave at the ith section.

Putting

$$X_i = \Gamma_i/\Gamma_o \tag{2}$$

where Γ_o is the maximum value among all (Γ_i)s so that $|X_i| \le 1$. With $\alpha = 0$, (1) can now be written as

$$\frac{\phi(f)}{FL} = \frac{\Gamma_o}{M}\frac{\sin\beta'(b/2)}{\beta'(b/2)}\sum_{i=1}^{M} X_i e^{-j[\beta' b(i-1/2)]} \tag{3}$$

$$= \frac{\Gamma_o \sin\beta'(b/2)}{M\beta'(b/2)}(A - jB) \tag{4}$$

where

$$A = \sum_{i=1}^{M} X_i \cos[\beta' b(i-1/2)] \tag{5}$$

$$B = \sum_{i=1}^{M} X_i \sin[\beta' b(i-1/2)] \tag{6}$$

$$\phi = \tan^{-1}(B/A). \tag{7}$$

Putting $\theta = \beta' b$, the phase difference between the microwave and optical wave after passing through from one of the section to the other is represented by (4), which can now be written as

$$\frac{\phi(f)}{FL\Gamma_o} = F(\theta). \tag{8}$$

That is, $F(\theta)$ is a function of the microwave frequency. The modulus of the complex function $F(\theta)$ is the frequency response of the modulus of the normalized phase modulation index.

Now, let us consider a rectangular frequency response. It is ideal if

$$|F(\theta)| = \begin{bmatrix} C_M, & \text{for } \theta \le \beta_1' b \\ 0, & \text{for } \theta \le \beta_1' b \end{bmatrix}. \tag{9}$$

From (4), (8), and (9)

$$F^2(\theta) = \frac{1}{M^2}\frac{\sin^2(\theta/2)}{(\theta/2)^2}(A^2 + B^2)$$

$$= \frac{2(1-\cos\theta)}{M^2\theta^2}\left[D_o + \sum_{i=1}^{M-1} 2D_i\cos(i\theta)\right]$$

$$= \frac{2}{M^2\theta^2}\left[G_o + \sum_{i=1}^{M} G_i\cos(i\theta)\right] \tag{10}$$

where

$$\begin{bmatrix} G_o \\ G_1 \\ \vdots \\ G_i \\ \vdots \\ G_{M-1} \\ G_M \end{bmatrix} = \begin{bmatrix} D_o - D_1 \\ -(D_o - 2D_1 + D_2) \\ \vdots \\ -(D_{i-1} - 2D_i + D_{i+1}) \\ \vdots \\ -(D_{M-2} - 2D_{M-1}) \\ -D_{M-1} \end{bmatrix} \tag{11}$$

$$\begin{bmatrix} D_o \\ D_1 \\ \vdots \\ D_i \\ \vdots \\ D_{M-1} \end{bmatrix} = \begin{bmatrix} \sum_{i=1}^{M} X_i^2 \\ \sum_{i=1}^{M-1} X_i X_{i+1} \\ \vdots \\ \sum_{i=1}^{M-i} X_i X_{i+1} \\ \vdots \\ X_1 X_M \end{bmatrix}. \tag{12}$$

Expanding θ^2 by Fourier series in the region $|\theta| \le \beta_1' b$, it gives

$$\theta^2 = \frac{(\beta_1' b)^2}{3} - \frac{4(\beta_1' b)^2}{\pi^2}\left[\sum_{n=1}^{\infty}(-1)^{n+1}\frac{1}{n^2}\cos\frac{n\pi\theta}{\beta_1' b}\right]. \tag{13}$$

As $F^2(\theta) = C_M^2$ for $\theta \le \beta_1' b$ and for the case $\beta_1' b = \pi$, (10) can be written as

$$C_M^2 M^2\left[\frac{\pi^2}{3} - 4\sum_{n=1}^{\infty}\frac{(-1)^{n+1}}{n^2}\cos(n\theta)\right]$$

$$= 2\left[G_o + \sum_{n=1}^{M} G_n\cos(n\theta)\right]. \tag{14}$$

By comparing the coefficients of $\cos(n\theta)$, a system of second-order nonlinear equations with M elements $X_1, X_2, \cdots, X_M$ can be obtained. For $n \le (M-1)$, see (15), shown at the bottom of the page. For each value of M, the values of X_i can be obtained from (15). The overlap integral Γ_i for each section of the electrode can then be calculated from (2). Hence, the frequency response and the half-wave voltage of the traveling-wave integrated electro-optic modulator can be computed.

IV. Numerical Solutions

Equation (15) represents a set of second-order nonlinear equations with M elements. For each value of M, several groups of real roots

$$\begin{bmatrix} \sum_{i=1}^{M} X_i^2 - \sum_{i=1}^{M-1} X_i X_{i+1} \\ \sum_{i=1}^{M} X_i^2 - 2\sum_{i=1}^{M-1} X_i X_{i+1} + \sum_{i=1}^{M-2} X_i X_{i+2} \\ \vdots \\ \sum_{i=1}^{M-(j-1)} X_i X_{i+(j-1)} - 2\sum_{i=1}^{M-j} X_i X_{i+1} + \sum_{i=1}^{M-(j+1)} X_i X_{i+(j+1)} \\ \vdots \\ \sum_{i=1}^{2} X_i X_{i+(M-2)} - 2X_1 X_M \end{bmatrix} = \begin{bmatrix} \pi^2 C_M^2 M^2/6 \\ 2C_M^2 M^2 \\ \vdots \\ 2(-1)^{j+1} C_M^2 M^2/j^2 \\ \vdots \\ 2(-1)^M C_M^2 M^2/(M-1)^2 \end{bmatrix} \tag{15}$$

TABLE I
THE VALUES OF X_i FOR $M = 3, 5, 7, 9, 13,$ AND 14

	M = 3	M = 5	M = 7	M = 9	M = 13	M = 14
X_1	1	0.2366	-0.1236	0.1602	0.3527	0.3623
X_2	-0.1366	0.4858	0.3210	0.4525	1	-0.6611
X_3	0.1040	1	-0.7182	0.7840	0.9699	1
X_4	-	-0.7264	1	0.5125	-0.2315	-0.7991
X_5	-	0.2717	-0.6998	-0.2099	-0.5602	0.0108
X_6	-	-	-0.9716	-0.7365	0.4431	0.9373
X_7	-	-	-0.4397	1	0.2285	0.8681
X_8	-	-	-	-0.5864	-0.7660	0.1770
X_9	-	-	-	0.1888	0.9226	-0.0709
X_{10}	-	-	-	-	-0.7311	-0.0387
X_{11}	-	-	-	-	0.4477	0.0049
X_{12}	-	-	-	-	-0.1919	-0.0626
X_{13}	-	-	-	-	0.0636	-0.0703
X_{14}	-	-	-	-	-	-0.0424

X_i $(i = 1, 2, \cdots, M)$ can be obtained. Here

$$X_i = a_i C_M M.$$

In each group of solutions, there exists a root of maximum absolute value $|X_i| = |X|_{\max}$.

In the design of the electrodes, this root was chosen as equal to one. That is,

$$|X|_{\max} = |a|_{\max} C_M M = 1. \tag{16}$$

Hence, the overlap integral, Γ_i, of each section of the electrode can be obtained as follows:

$$\Gamma_i = X_i \Gamma_o = \frac{a_i}{|a|_{\max}} \Gamma_o. \tag{17}$$

Using the Newton's iteration method to solve (15) and finding out the maximum absolute value, the values of X_i are obtained. Table I shows the respective values of X_i when $M = 3, 5, 7, 9, 13,$ and 14.

V. FREQUENCY RESPONSE

The length of each section of the electrode is given by $b = L/M$ where L and M have been defined in Section II. For the case of $\beta_1' b = \pi$, where $\beta_1' = 2\pi(f_1)(n_m - n_o)/c$, and for an M-section electrode system, there will be a common cutoff frequency, f_c, which is given by

$$f_c = \frac{c}{2(n_m - n_o)b}. \tag{18}$$

Equation (18) shows that the upper cutoff frequency of the modulator depends only on the length, b, of each section of the electrode and the velocity mismatch $(n_m - n_0)$. It is independent of the number of sections M. The frequency responses of an electro-optic modulator with the length of each electrode section equals to 1 mm are plotted in Fig. 2 for $M = 1, 3, 5, 7, 9, 13,$ and 14. In Fig. 2, it is obvious that modulators with different values of M have the same bandwidth if the length of each section of electrode is equal. For the case $M = 5$, it can be shown that when the overlap integral factors vary $\pm 10\%$ from the ideal parameters as set in Table I, the flatness of the frequency response only changes from -0.525 dB to $+0.463$ dB. Concerning the microwave loss, this can be reduced to 0.5 dB/(cm·GHz$^{1/2}$) in the "real world." Some can even be lowered to 0.24 dB/(cm·GHz$^{1/2}$). In this case, the variation of the frequency response will be less than ± 0.5 dB. Therefore, the assumption of $\alpha = 0$ can be made.

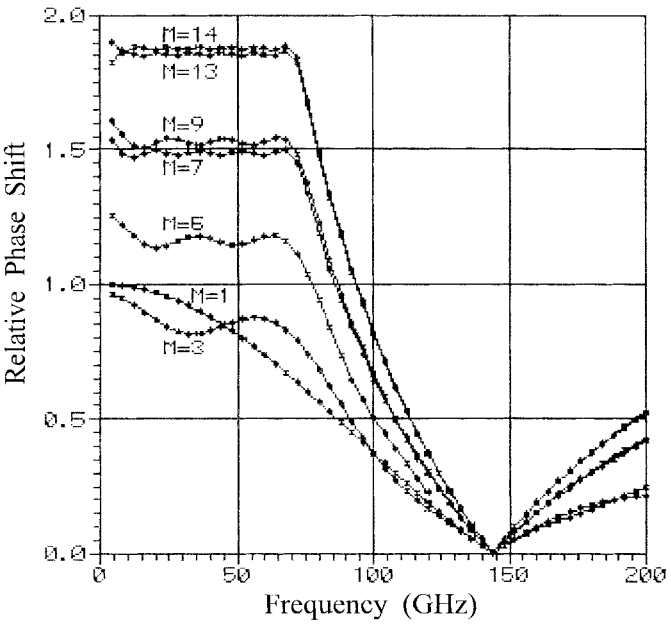

Fig. 2. Calculated frequency response of an electrooptic modulator with phase reversal electrode and with step electrode length equal to 1 mm.

VI. HALF-WAVE VOLTAGE AND BVR

In (3), when $\beta' b = 0$, that is, a dc voltage is applied to the electrode, the normalized phase shift would be

$$F(0) = \frac{\phi(0)}{FL\Gamma_o} = \frac{1}{M} \sum_{i=1}^{M} X_i = C_M \sum_{i=1}^{M} a_i. \tag{19}$$

For a conventional electrode with length L equals to b, the voltage needed for a phase change of π radians in the optical wave is

$$(V_\pi)_1 = \frac{\pi G}{F_1 b \Gamma_o} \tag{20}$$

where $F_1 = FG/V$.

For an M-sectioned electrode, if the length of each section is b (equals to L/M) with the design satisfies (17), the voltage needed for a phase shift of π radians in the optical wave can be obtained from (19) and is simplified as

$$(V_\pi)_M = \left[\frac{\pi G}{F_1 b \Gamma_o}\right] \Big/ \left[C_M M \sum_{i=1}^{M} a_i\right]. \tag{21}$$

It follows from (16), (18), (20), and (21) that the figure of merit, Q, for an electrooptic modulator with M sections of electrodes is

$$\begin{aligned} Q &= \frac{f_1/(V_\pi)_M}{f_1/(V_\pi)_1} = \frac{(V_\pi)_1}{(V_\pi)_M} = C_M M \sum_{i=1}^{M} a_i \\ &= \left(\sum_{i=1}^{M} a_i\right) / |a|_{\max} = \sum_{i=1}^{M} X_i \end{aligned} \tag{22}$$

where Q has been defined in Section I.

VII. OPTIMIZATION OF THE FIGURE OF MERIT, Q

For a conventional modulator with $M = 1$ and from (1) and (20), $(V_\pi)_1$ can be rewritten as

$$(V_\pi)_1 = \frac{-\lambda G}{n_o^3 r \Gamma L}. \tag{23}$$

Equation (23) shows that $(V_\pi)_1$ can be reduced by increasing the length L. However, (18) indicates that increasing the length b

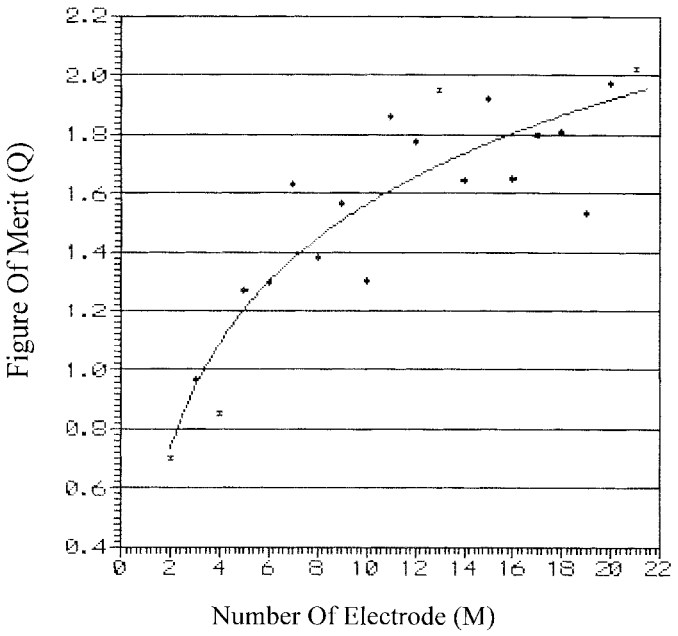

Fig. 3. The figure of merit versus the number of electrodes for a phase-reversal modulator.

will decrease the bandwidth of the modulator (as the upper cutoff frequency, f_c, decreases with increasing the electrode length L). Hence, there is a tradeoff between $(V_\pi)_1$ and f_c.

From (18) and (23), the BVR for a conventional modulator is expressed as

$$(BVR)_1 = \frac{cn_o^3 r\Gamma_1}{2(n_m - n_o)\lambda G}. \tag{24}$$

It is obvious that $(BVR)_1$ is independent of the length of the electrode L. Hence, it is impossible to increase the $(BVR)_1$ by adjusting only L. In electrooptic modulator with step phase reversal electrodes, the $(BVR)_M$ can be deduced from (22) as follows:

$$(BVR)_M = Q \cdot (BVR)_1. \tag{25}$$

From (15), it can be shown that

$$\sum_{i=1}^{M} a_i = \left\{ M^2 \left[\frac{\pi^2}{6} - 2\left(1 - \frac{1}{2^2} + \cdots + \frac{(-1)^M}{(M-1)^2}\right)\right] + 2\,\mathrm{Code}(M) \right\}^{1/2} \tag{26}$$

where

$$\mathrm{Code}(M) = 0 \quad \text{when } M \text{ is odd}$$

and

$$\mathrm{Code}(M) = 1 \quad \text{when } M \text{ is even.}$$

$\sum_{i=1}^{M} a_i$ has a value of around one. When M is odd, its value is greater than one. When M is even, its value is less than one. Hence, from (22), an electrooptic modulator with odd-numbered sections of electrodes will have a larger value of Q. For each value of M, there are several groups of real roots X_i in (15). In order to obtain the maximum value of Q for each M, a group of real roots with minimum $|a|_{\max}$ values are required

$$|a|_{\max} = |X|_{\max}/C_M M.$$

Fig. 3 plots the maximum value of Q for each M versus the number of electrode sections M. In Fig. 3, it is obvious that Q is greater than 1 when $M > 4$. $(\mathrm{BVR})_M$ is greater than $(\mathrm{BVR})_1$ for $M > 4$. This means that for $M > 4$, the $(V_\pi)_M$ required by the modulator with M-sections of electrode is lower than $(V_\pi)_1$ required by a conventional modulator of the same bandwidth. The figure of merit, Q, is saturating at a value of approximately two for 12 to 21 electrode sections. With the observation that Q is higher when M is odd, we can choose $M = 7, 11,$ and 13, etc. in the design of phase-reversal modulators.

VIII. Conclusion

The phase-reversal step electrode structure of an electrooptic modulator with flat frequency response can be designed with different overlap integrals that satisfy (15). Their real roots X_i can be solved numerically. From Fig. 2, the flatness of the frequency response shows significant improvement as M increases. At frequencies less than 72 GHz, the flatness of the curves is within $\pm$ 0.3 dB. For modulators of the same bandwidth but with different values of M, the relative phase shifts are different. When M increases, the relative phase shift increases. This implies that V_π is lowered as M increases. From Fig. 3, the figure of merit, Q, increases as M increases. When $M = 5, 7, 9, 13,$ and 21, the BVR's increase by 1.268, 1.632, 1.565, 1.950, and 2.022 times that of the BVR with M equals to one, respectively.

References

[1] W. R. Leeb, A. L. Scholtz, and E. Bonek, "Measurement of velocity mismatch in traveling-wave electrooptic modulators," *IEEE J. Quantum Electron.*, vol. QE-18, pp. 14–16, June 1982.

[2] R. C. Alferness, S. K. Korotky, and E. A. Marcatili, "Velocity-matching techniques for integrated optic traveling wave switch/modulators," *IEEE J. Quantum Electron.*, vol. QE-20, pp. 301–309, Feb. 1984.

[3] H. Y. Chung, W. S. C. Chang, and E. L. Adler, "Modeling and optimization of traveling-wave $LiNbO_3$ interferometric modulators," *IEEE J. Quantum Electron.*, vol. 27, no. 3, pp. 608–617, Mar. 1991.

[4] D. W. Dolfi, M. Nazarathy, and R. L. Jungerman, "40 GHz electro-optic modulator with 7.5 V drive voltage," *Electron. Lett.*, vol. 24, no. 9, pp. 528–529, Apr. 1988.

[5] G. K. Gopalakrishnan *et al.*, "40 GHz, low half-wave voltage Ti:$LiNbO_3$ intensity modulator," *Electron. Lett.*, vol. 28, no. 9, pp. 826–827, Apr. 23, 1992.

[6] K. Noguchi *et al.*, "75 GHz broadband Ti:$LiNbO_3$ optical modulator with ridge structure," *Electronics Letters*, vol. 30, no. 12, pp. 949–951, June 9, 1994.

[7] D. Erasme, D. A. Humphreys, A. G. Roddie, and M. G. F. Wilson, "Design and performance of phase reversal traveling wave modulators," *J. Lightwave Technol.*, vol. 6, pp. 933–936, June 1988.

[8] D. Erasme and M. G. F. Wilson, "Analysis and optimization of integrated travelling-wave modulators using periodic and nonperiodic phase reversals," *Optical and Quantum Electronics*, vol. 18, pp. 203–211, Feb. 1986.

[9] W. K. Burns, "Analytic output expression for integrated optic phase reversal modulators with microwave loss," *Appl. Opt.*, vol. 28, pp. 3280–3283, Aug. 1989.

[10] K.-W. Hui, Y.-M. Choi, B.-Y. Wu, and Z.-H. Zhang, "Design of wide bandwidth electrode system in travelling wave integrated optic modulator," presented at Asia–Pacific Microwave Conference, Oct. 10–13, 1995.